Comsolic solution of an elliptic cylindrical compressible fluid flow

Azad Hussain (azad.hussain@uog.edu.pk)
University of Gujrat
Ali Hassan
University of Gujrat
Mubahar Arshad
University of Gujrat

Research Article

Keywords: viscous compressible, elliptical cylinder, water based, nanofluid.

Posted Date: April 16th, 2021

DOI: https://doi.org/10.21203/rs.3.rs-386340/v1

Version of Record: A version of this preprint was published at Scientific Reports on October 8th, 2021. See the published version at https://doi.org/10.1038/s41598-021-99138-7.

Comsolic solution of an elliptic cylindrical compressible fluid flow

Azad Hussain [a],[1] Ali Hassan[a], Mubahar Arshad [a]
[a] Department of Mathematics, University of Gujrat , Gujrat, 50700 Pakistan

Abstract: In the present study, viscous compressible flow with heat transfer effects in high permeable elliptical cylinder is investigated. Flow is kept laminar through Reynolds number at about 100. The heat transfer in fluids physics has been chosen to couple with laminar flow. The time dependent outcomes of surface velocity, pressure distribution, temperature distribution, isothermal contour profiles and drag coefficient are discussed in results. The mesh created through COMSOL has been described statistically. This mathematical modeling of stated problem is done in COMSOL Multi-physics. The results will help greatly to understand characterizations of viscous fluids.

Article Highlights

- The mathematical modeling of the viscous compressible water based laminar flow is done in COMSOL multi-physics.
- The time dependent outcomes are discussed, the heat transfer feature is coupled with laminar flow.
- The results will help in understanding the compressible attributes of fluids as well as the characterizations of viscous fluids.

Keywords: viscous compressible, elliptical cylinder, water based, nanofluid.

1. Introduction:

The boundary layer flow of Eyring Powell model fluid with variable viscosity over a stretching cylinder has been discussed for incompressible fluid by M.Y.Malik, A.Hussain and S.Nadeem [1]. Three dimensional stagnation point flow of hybrid nanofluid over a circular cylinder has been studied by S. Nadeem, Nadeem Abbas and A.U. Khan [2], the radii of cylinder was varying sinusoidally. The heat transfer with boundary layer flow for second grade fluid over a cylinder has been discussed by S. Nadeem, Abdul Rehman, Changhoon Lee and Jinho Lee [3]. Exponentially vertical stretching cylinder for hyperbolic tangent flow has been discussed for boundary layer flow by Muhammad Naseer, Muhammad Yousaf Malik, Sohail Nadeem and Abdul Rehman [4]. The temperature dependent viscosity for boundary layer flow of Walter's B fluid for stretching cylinder has been studied by Azad Hussain and Anwar Ullah [5]. The stagnation point MHD flow past a shrinking/stretching sheet for casson fluid has been discussed for variable viscosity by Azad Hussain, Sana Afzal, Rizwana Rizwana and M.Y.Malik[6]. The viscoelastic nanofluid under the effect of radiation has been discussed for incompressible fluid by Azad Hussain, Lubna Sarwar and Sohail Nadeem [7]. The heat transfer analysis for three dimensional stagnation point flow over exponentially stretching sheet has been studied by Fiaz Ur Rehman , S. Nadeem , R.U. Haq [8].
Viscous flow over a non-linearly stretching sheet has been studied by K. Vajravelu [9]. Three dimensional viscous supersonic flow over a cone at incidence has been studied by A. Lin and S.G. Rubin [10]. E. R. VAN DRIEST [11] has studied stability of

boundary layer of compressible fluid flow on a flat plate along with heat transfer effects. Incompressible fluids have been studied by numerous researchers but there are very few article available for compressible fluid flow study. M. R. Malik and R. E. SPALL has discussed compressible fluid flow for axis-symmetric bodies for fluid stability[12]. Heat and mass transfer for visco-elastic flow for flat plate and a cone under MHD influence have been studied by B. Rushi Kumar and R. Sivaraj [13]. Brain J. Cantwell [14] has elaborated compressible flow in two dimensional flow in his book "Fundamentals of compressible flow" in depth. A numerical investigation of non-Newtonian fluid for laminar flow with heat transfer feature in porous medium for microbial fuel cell array are recently published on laminar flow [15], [16]. There is a urgent need to study mathematical modelling of viscous compressible flow to find out its various applications. Through mathematical modelling the real life problems can be modeled. COMSOL, enables us with its features to study fluid flow for low mac numbers or for compressible fluids, multi-channel vacuum and complex urban flow has been modeled and studied through COMSOL in[17], [18].
Numerical investigation of the lift and drag coefficient for marine riser at high Reynolds number has been discussed by [19]. W Frohlingsdorf and H Unger [20] has studied compressible flow and energy separation for Ranque-Hilsch vortex tube numerically. Tim colonius [21] has thoroughly discussed modeling artificial boundary conditions for compressible flow. The numerical investigation of compressible flow through a chimney [22] has been done by Xinping zhou and Jiakuan yang. Another monograph has been studied on magneto-viscous effects by Odenbach [23]. The effect of magnetization force on the rotating disk in the ferrofluid flow is studied by Anupam Bhandari [24]. The effects of stationary magnetic field on ferrofluid past through a cylinder is studied by Anupum Bhandari [25]. Physiological flow of biomedical compressible fluids inside a ciliated symmetric channel [26] has been investigated by S. Nadeem and Aleesha Qaiser.
The purpose of this article is to investigate the laminar flow of viscous compressible fluid that is dependent of time. The laminar flow is coupled with heat transfer feature. The mathematical modeling of elliptic cylindrical flow is done in COMSOL. The outcomes are discussed for velocity, pressure temperature and isothermal temperature distribution. The mesh created through COMSOL has been described with comprised constitutes. The thermophysical properties of water based fluid that has been utilized are elaborated.

2. Mathematical Formulation

The sketch of flow region is given below. First of all, a rectangular geometry is drawn in the COMSOL with specifics as 2.0 m in width and 0.4 m in height with coordinates position as (r,z) (0,0). An ellipse is drawn at coordinates position (0.3,0.2), with (0.15,0.05) being major and minor axis. The difference of both geometrical shapes is taken through boolean and partition section and then through building all command final geometry is obtained. The physics of heat transfer in fluids is added in COMSOL, in the initial values the temperature is taken 200 K, temperature 1 (taken 298 K on the upper boundary) and temperature 2 (taken 300.5 K on lower boundary) are added under heat transfer segment. The fluid properties of thermal conductivity, fluid density, specific heat at constant pressure and specific heat ratio are added.

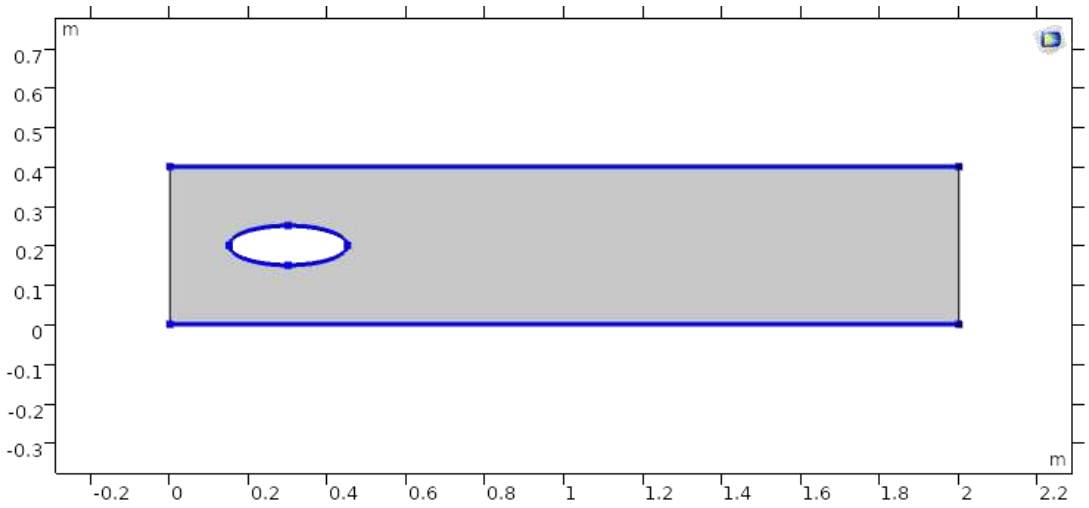

Fig. 1 The sketch of two dimensional elliptic cylindrical flow.

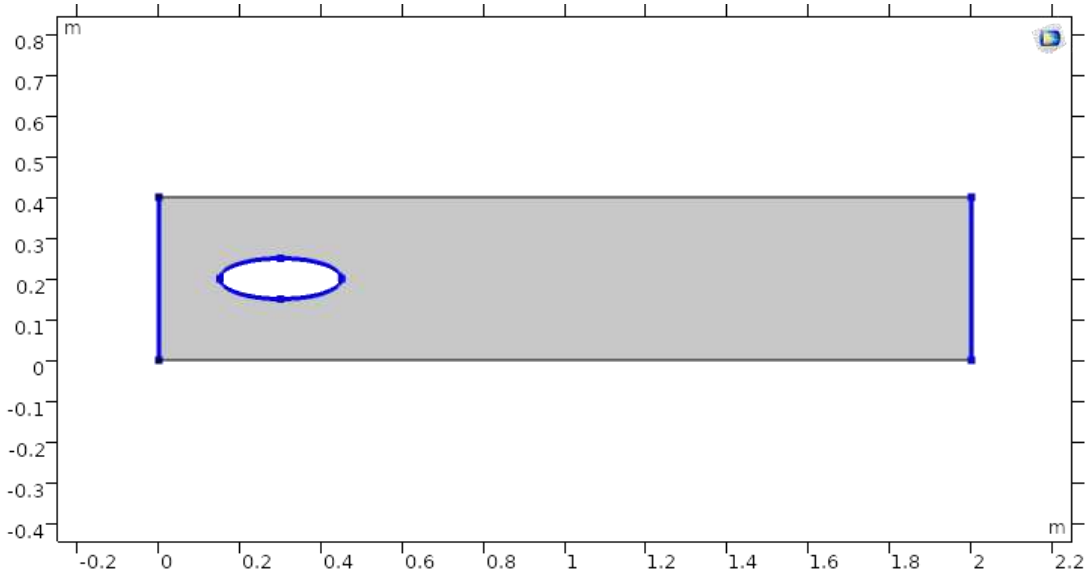

Fig. 2 The sketch of thermal isolated boundary of two dimensional elliptic cylindrical flow.

In the next step, properties of fluid have been added from material properties.
The model governing equations are as fellow :
The momentum equation is given as

$$\rho\frac{\partial u}{\partial t}+\rho(u.\nabla)u=-\nabla(pI)+\nabla K+F_b\,, \qquad (1)$$

the equation of continuity is

$$\frac{\partial \rho}{\partial t}+\nabla.(\rho u)=0, \qquad (2)$$

as the model is coupled with the heat transfer, the governing equation for heat transfer is given as:

$$d_z\rho c_p\left(\frac{\partial T}{\partial t}\right) + d_z\rho c_p(u\nabla T) + \nabla q = d_z Q + q_0 + d_z Q_p + d_z Q_{vd}\,, \qquad (4)$$

where the relation consist of following expressions:

$$Q = 0, q_0 = \frac{q}{A_s \Delta T},\ \ Q_p = \alpha_p T\left(\frac{\partial P}{\partial t} + u\nabla P\right),\ \text{and}\ Q_{vd} = \tau.\nabla u\,, \qquad (5)$$

where, $q = -k\nabla T,\ \alpha_p = \frac{-1}{\rho}\frac{\partial P}{\partial T}$ and also $\tau = -pI + \mu A_1, \tau_{race}(\tau.\nabla u) = \tau.\nabla u$

and $A_1 = ((\nabla u) + (\nabla u^T)),\ \ \Delta T = T_1 - T_2\,,\ A_s = 0.8m^2\,, d_z = 1m$ (thickness) .

The body forces are neglected the momentum, continuity and heat transfer equations will reduces to

$$\frac{\partial \rho}{\partial t} + \rho\left(\frac{\partial u_r}{\partial r} + \frac{u_r}{r} + \frac{\partial u_z}{\partial z}\right) = 0, \qquad (6)$$

$$\left[\frac{\partial u_r}{\partial t} + u_r\frac{\partial u_r}{\partial r} + u_z\frac{\partial u_r}{\partial z} - \frac{u_\theta^2}{r}\right] = -\frac{-1}{\rho}\frac{\partial P}{\partial r} + \nu\left[2\frac{\partial^2 u_r}{\partial r^2} + \frac{\partial^2 u_r}{\partial r \partial z} + \frac{1}{3}\frac{\partial^2 u_r}{\partial z^2}\right], \qquad (7)$$

$$\left[\frac{\partial u_\theta}{\partial t} + u_r\frac{\partial u_\theta}{\partial r} + u_z\frac{\partial u_\theta}{\partial z} + \frac{u_\theta u_r}{r}\right] = \nu\left[\frac{1}{3}\frac{\partial^2 u_\theta}{\partial r^2} - \frac{1}{r}\frac{\partial u_\theta}{\partial r}\right) + \frac{1}{3}\frac{\partial^2 u_\theta}{\partial z^2}\right], \qquad (8)$$

$$\left[\frac{\partial u_z}{\partial t} + u_r\frac{\partial u_z}{\partial r} + v_z\frac{\partial u_z}{\partial z}\right] = -\frac{-1}{\rho}\frac{\partial P}{\partial z} + \nu\left[\frac{1}{3}\frac{\partial^2 u_z}{\partial r^2} + \frac{\partial^2 u_r}{\partial z \partial r} + 2\frac{\partial^2 u_z}{\partial z^2}\right], \qquad (9)$$

at variable pressure:

$$\rho c_p\left(\frac{\partial T}{\partial t} + T\nabla u\right) - k\nabla^2 T = \frac{q}{A_s \Delta T} - \frac{1}{\rho}\frac{\partial p}{\partial t}\frac{\partial t}{\partial T}\left(\frac{\partial p}{\partial t} - p\nabla u\right) + (-pI + \mu A_1)\nabla u, \qquad (10)$$

at constant pressure:

$$\rho c_p\left(\frac{\partial T}{\partial t} + T\nabla u\right) - k\nabla^2 T = \frac{q}{A_s \Delta T} + \mu A_1(\nabla u), \qquad (11)$$

$$\begin{aligned} Pr(\theta'') = \nu\Big(&\frac{1}{2}\theta'\eta + 2\theta s\Big) \\ &- pr\frac{Gv}{K(T_w - T_\infty)}\Bigg[\frac{q_0}{A_s \Delta T} \\ &+ \Bigg\{\mu\Bigg(\frac{\partial^3}{\partial r^3}\left(\frac{4}{3}u_r + u_\theta + u_z\right) + \frac{1}{3}\mu\frac{\partial^2}{\partial r^2}\left(\frac{u_\theta}{r} + \frac{\partial u_r}{\partial z}\right) - \frac{\partial u_\theta}{\partial z}\left(p - \frac{4}{3}\mu - \frac{1}{3}\frac{\partial u_z}{\partial z}\frac{\partial u_\theta}{\partial z}\right) \\ &- \frac{\partial u_\theta}{\partial z}\left(\frac{1}{3}\frac{\partial u_r}{\partial z} - \frac{u_\theta}{r}\right) - \frac{u_r}{r}\left(p - \frac{4}{3}\mu\frac{u_r}{r}\right) - \mu\frac{u_\theta}{r}\left(\frac{1}{3}\frac{\partial u_\theta}{\partial r} - \frac{u_\theta}{r}\right) \\ &- p\frac{\partial u_r}{\partial r}\Bigg)\Bigg\}\Bigg]. \end{aligned} \qquad (12)$$

The similarity transformation for heat transfer equation is

$$\mathrm{T(t,r,z)} - \mathrm{T}_\infty = (T_w - T_\infty)\theta,\ T_w - T_\infty = (T_0 - T_\infty)\frac{x}{L}(1 - st^*)^{-2}, t^* = (\Omega sin\alpha^*)t, \quad (13)$$

where $\eta = \frac{\mathrm{z}\,(\Omega \mathrm{sin}\alpha^*)^{0.5}}{\mathrm{v}^{0.5}(1-\mathrm{st}\Omega \mathrm{sin}\alpha^*)^{0.5}}$, $\mathrm{G} = (\Omega \mathrm{sin}\alpha^*)^{-1}(1 - \mathrm{st}\Omega \mathrm{sin}\alpha^*)$, and $\mathrm{Pr} = \frac{\mathrm{K}}{\rho \mathrm{C_p}}$. (14)

Where, ρ is density of fluid, u is velocity of fluid , p denotes pressure, t represents time, μ is viscosity of fluid, ν is the kinematic viscosity, u_r, u_θ, u_z are the velocity components. In equation 4, c_p represent the specific heat at constant pressure, q denotes heat flux vector, ∇T represents temperature gradient, k denotes thermal conductivity, $\mathrm{d_z}$ is thickness of the geometry,η is the non-dimensional parameter, T is absolute temperature in kelvin, Q is heat source other then the viscous dissipation, $\mathrm{Q_{vd}}$ is the heat source via viscous dissipation, τ represents stress tensor, $\mathrm{A_s}$ represents area of heat transfer,T_w denotes wall temperature, T_∞ represents free stream velocity and ΔT denotes temperature difference. In other words the R.H.S of equation 4, actually represents the work done by pressure change, is result of heat under adiabatic compression as well as some thermo-acoustic effects, it is generally low for low number or for compressible fluid flow. See, the table 1,2,3 for thermophysical properties, mesh statistics and mesh quality respectively. Fig. 1 shows the boundary wall at which the velocity component is zero. The boundary conditions are considered and an inlet (entrance, outlet (exit) are selected in COMSOL. The physics of heat transfer is added through add-physics feature in the COMSOL, to solve Navier-stokes equations, the boundary conditions are as fellow:
Region “Domain”
Start “Outer”
the mirror conditions on the bottom boundary are:

$$u_r = u_\theta = u_z = 0\ and\ p = 0\ all\ Natural \qquad line\ to\ (0.4,0)$$

no Slip condition is considered (i.e, velocity=0)

$$\begin{cases} u_r = u_\theta = u_z = 0\ and\ p = 0\ all\ Natural & line\ to\ (0.4,2.0) \\ u_r = u_\theta = u_z = 0\ and\ p = 0\ all\ Natural & line\ to\ (0,2.0) \\ u_r = u_\theta = u_z = 0\ and\ p = 0\ all\ Natural & line\ to\ close \end{cases} \quad (15)$$

$$\begin{cases} u_r = u_\theta = u_z = 0\ and\ p = 0\ \ at\ t = 0 \\ \quad at \quad r = 0.4, z = 2.0\ , u = -\ U_0 n. \end{cases} \quad (16)$$

In equation (16), the U_0 represent the normal inflow velocity and n is the unit vector, the negative sign describes that flow is moving from higher concentration area to lower concentration area.

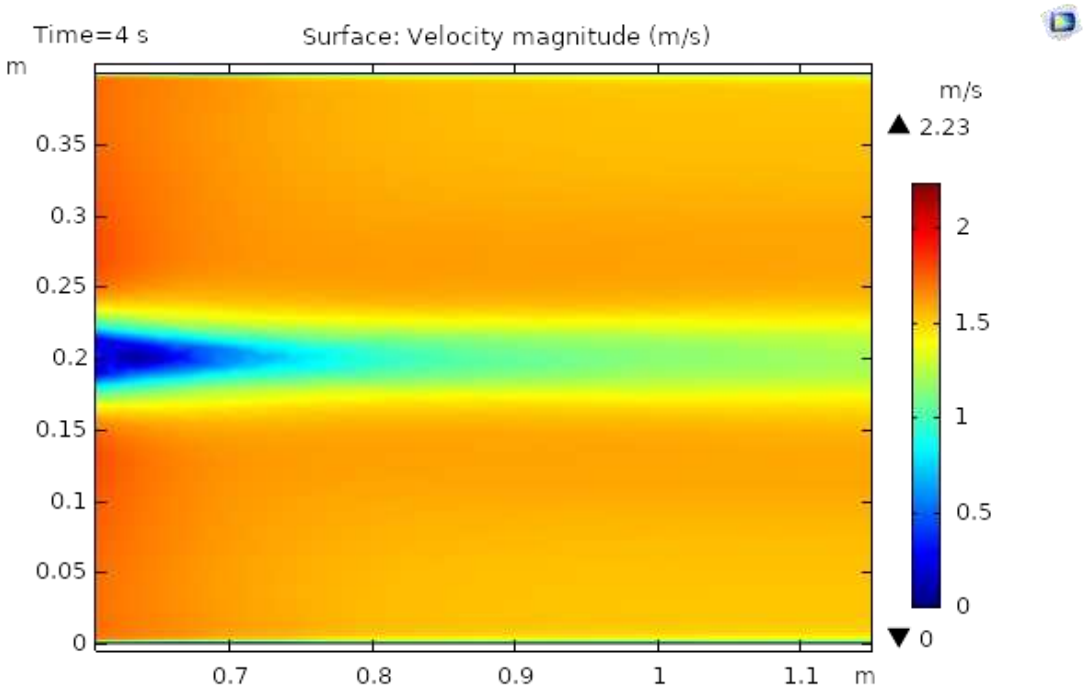

Fig. 3 The velocity distribution in two dimensional elliptic cylindrical flow at t=4s

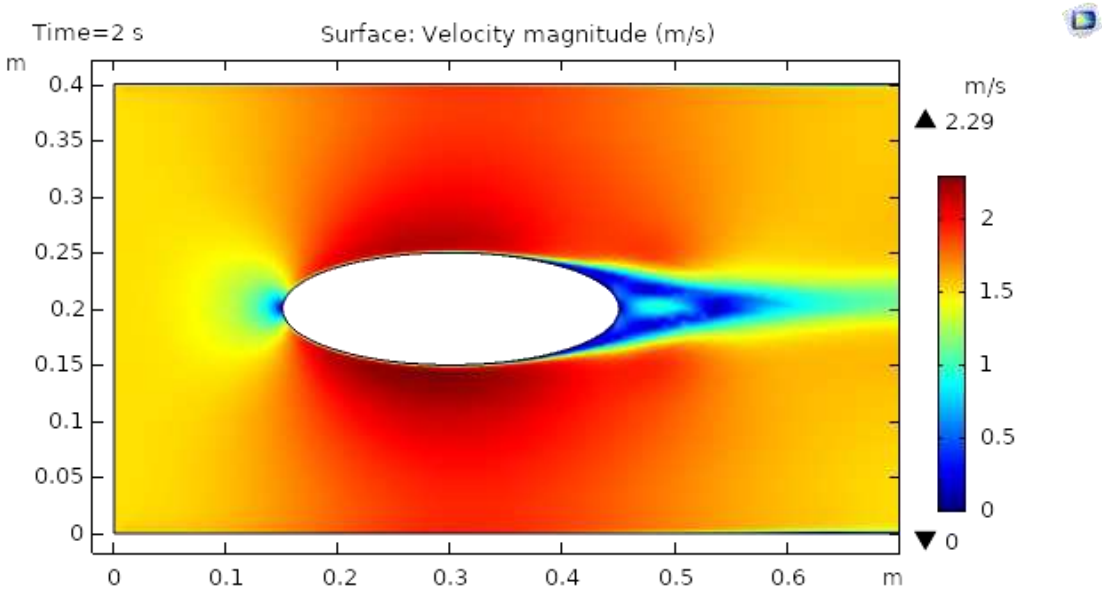

Fig . 4 The velocity distribution in two dimensional elliptic cylindrical flow at t=2s

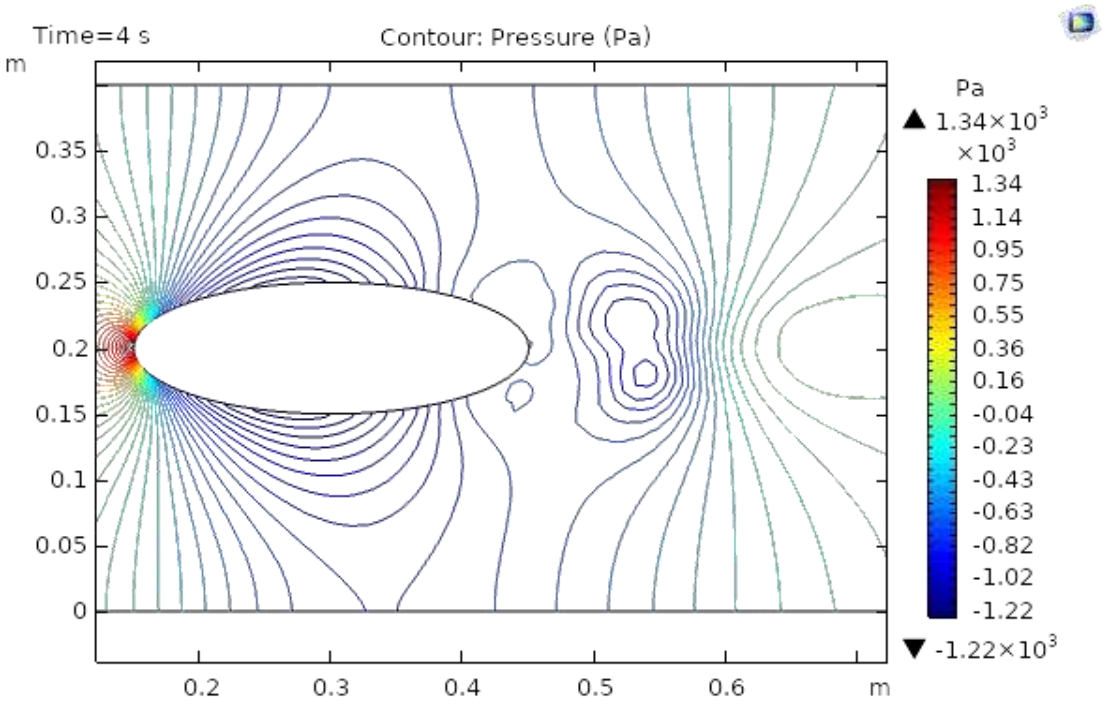

Fig. 5 Pressure distribution in two dimensional elliptic cylindrical flow at t=4s

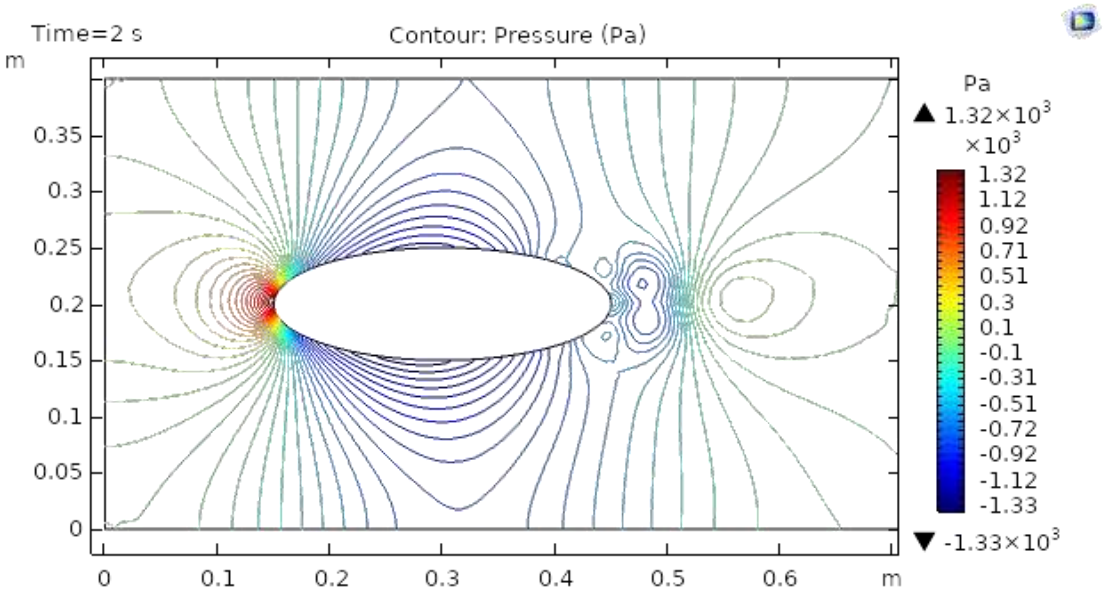

Fig. 6 The pressure distribution in two dimensional elliptic cylindrical flow at t=2s

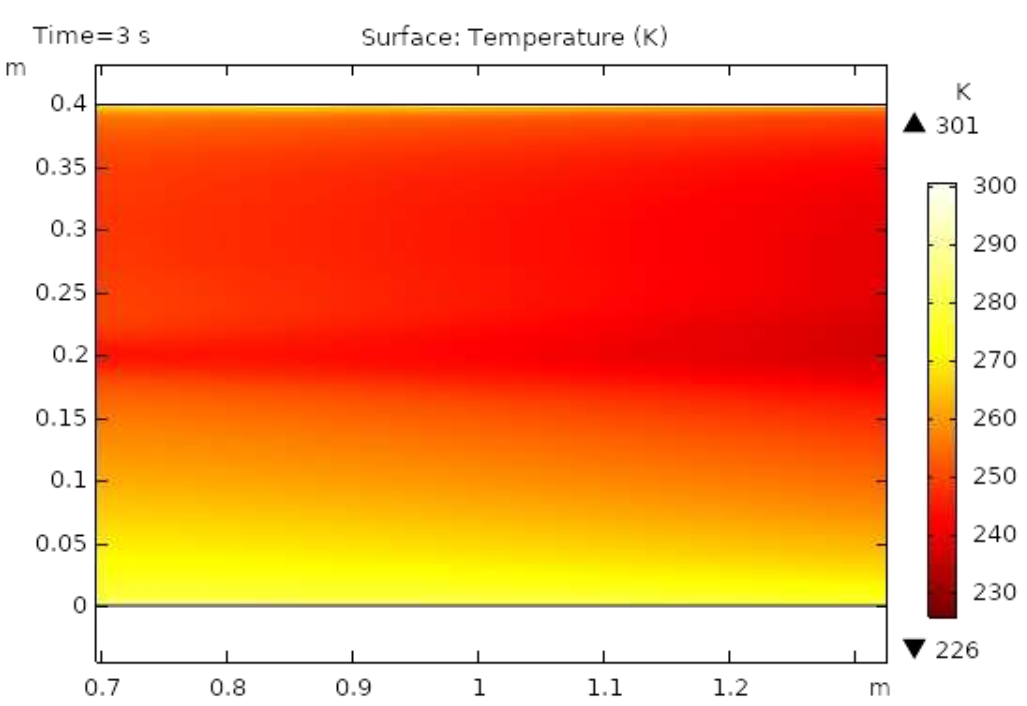

Fig. 7 Temperature distribution at t=3s

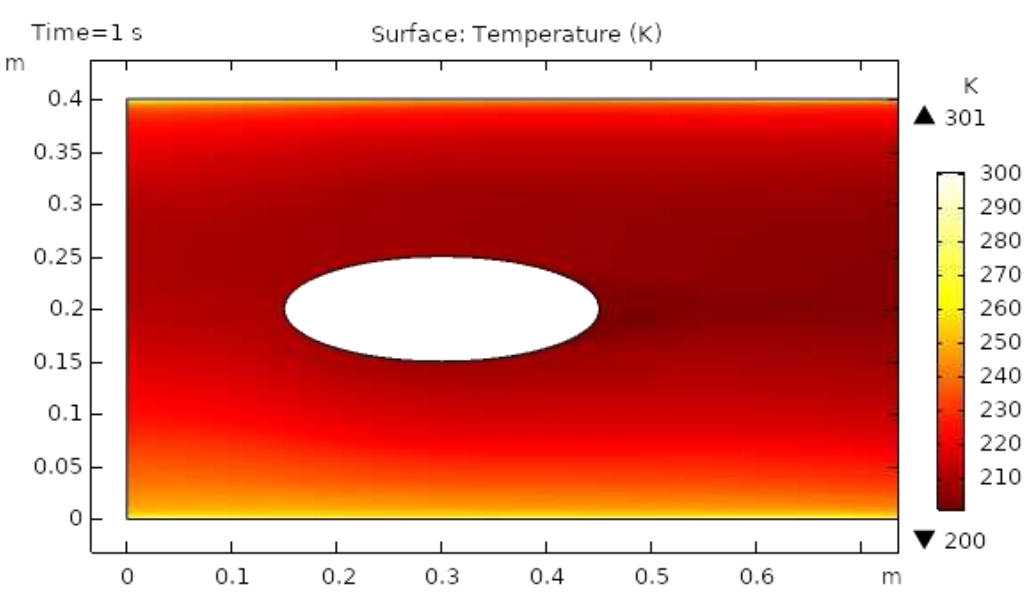

Fig. 8 Temperature distribution at t=1s

Table 1: The following parameters have been utilized in calculations:

Properties	Numeric Value	Description
Density	997 kg/m^3	Density of fluid
Temperature	20^0 C	Temperature of fluid
Dynamic Viscosity	8.90×10^{-4} m^2/s	Dynamic Viscosity of ferrofluid
Specific Heat Ratio	1.330	Specific Heat Ratio of fluid
Thermal Conductivity	0.613 K(W/m.K)	Thermal Conductivity of fluid
Temperature 1	298 (Kelvin)	Temperature of upper boundary
Temperature 2	300.5 (Kelvin)	Temperature of lower boundary
Size of particle	9 nanometer (nm)	Size of the particles in fluid

3. Solution of Problem:

The mesh is created through physics controlled finer option, the total number of triangular entities are 23858, Quadrilateral entities are 1804, edge entities are 986 and the vertex entities are 8. The maximum entity size taken is 0.014 and minimum entity size taken is 4E-4. Corner refinement in domain 1 is selected COMSOL and minimum angle between the boundaries is 240 degrees, sharp corners are handled through the trimming option in the COMSOL. This particular model is studied under the laminar category heat transfer feature. Finally, the model is simulated in COMSOL and the results are obtained.

Table 2: Mesh statistics description:

Property	Value
Minimum entity quality	0.3727
Average entity quality	0.8484
Triangular entities	23858
Quadrilateral entities	1804
Edge entities	986
Vertex entities	8

Table 3: Mesh size description:

Geometric Entity level	boundary
Calibrate for	Fluid dynamics
Selection	Boundaries 2-3, 5-8
Maximum entity size	0.014
Minimum entity size	4E-4
Curvature factor	0.3
The maximum entity growth	1.13

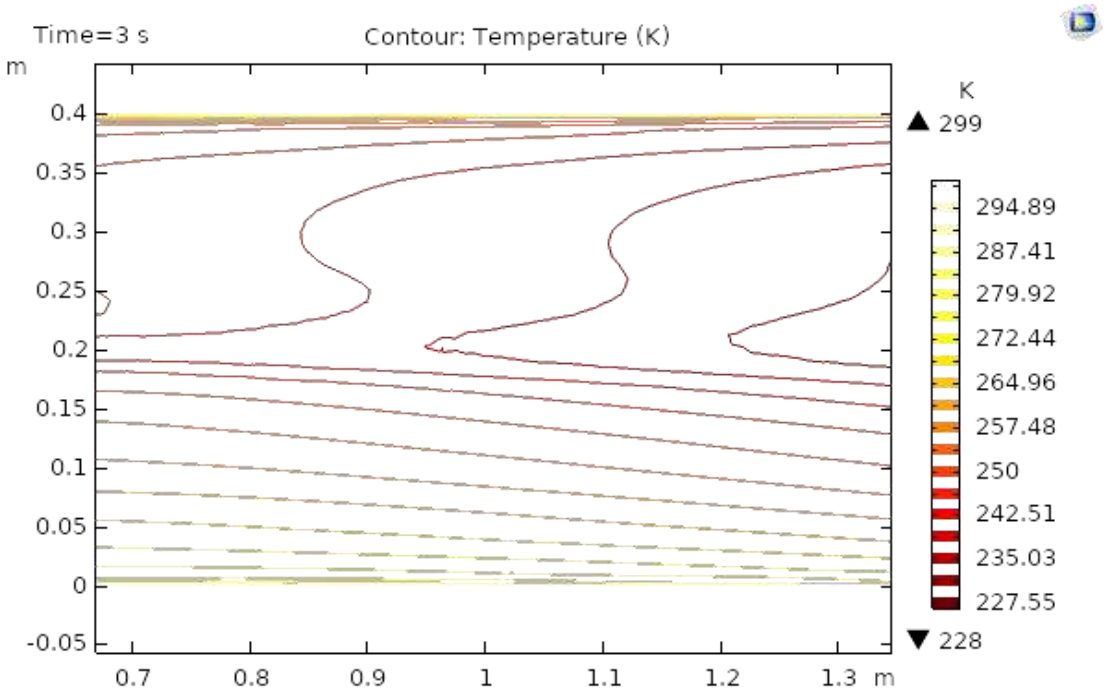

Fig. 9 Isothermal contour temperature distribution at t=3s

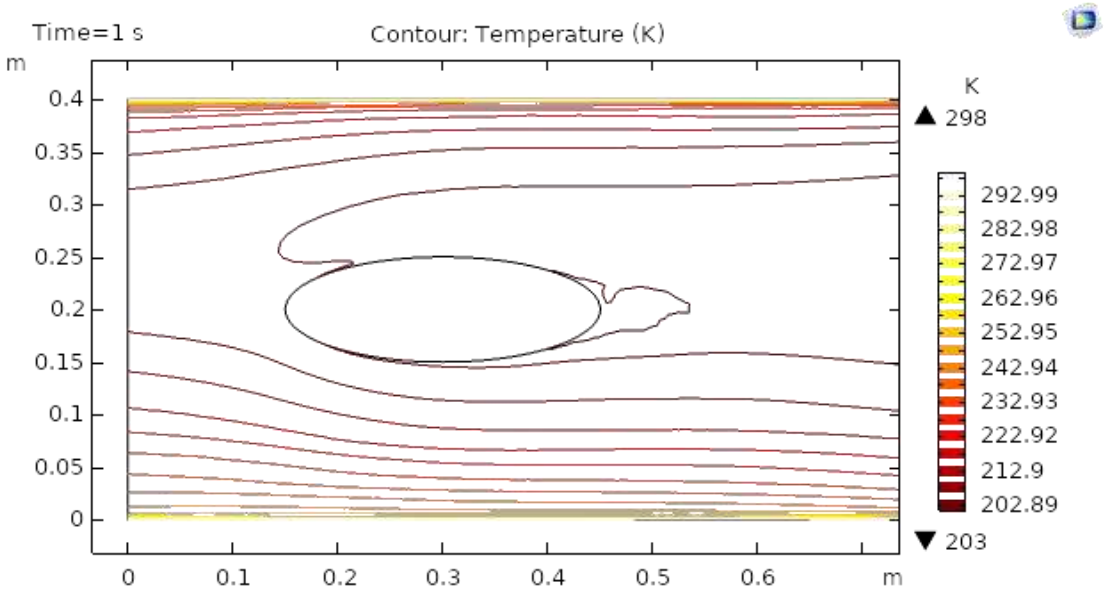

Fig. 10 The velocity distribution in two dimensional elliptic cylindrical flow at t=1s

The thermophysical properties that has been utilized for laminar flow and couples heat transfer are presented in table 1. The mesh constructed with help of COMSOL has number of geometric entities. Table 2, presents all those entities which have been created along with their quality and total number of different entities. The mesh is created for a particular section, applicable boundaries has been given, the maximum and minimum size of entities are presented in table 3.

4. Outcomes and discussion

Present outcome discusses laminar flow of viscous compressible fluid in elliptic cylindrical geometry (see) Fig. 1. The 2-dimensional model for laminar flow has been designed in the presence of heat transfer feature in COMSOL. In obtained two dimensional plots, vertical axis has been considered the diameter of ellipse and horizontal axis represents z-direction. The laminar flow is compressible and time dependent. Fig.1 describes the sketch of the drawn geometry for two dimensional elliptic cylindrical flow. Fig. 2 shows the isothermal boundary of geometry for heat transfer feature. Fig. 3 shows the velocity distribution at time 4 seconds, as we move away from our designed geometry the velocity profile stays constant at 1.5m/s and as we can see in center part the velocity is at 0.5m/s. The maximum value of velocity is at 4s is 2.23 m/s as shown in the figure. Fig. 4 describes the velocity distribution at time 2 seconds, it shows a distinct pattern, in this case the maximum value of velocity is 2.29 m/s if we vary the time parameter we can even get more distinct patterns, in the region around the elliptic cylinder the velocity is maximum while it is observed minimum at boundaries. Fig. 5 illustrates pressure distribution around elliptic cylinder a very distinct pattern can be seen at time 4s. Fig. 6 shows pressure contours for time 2s the pattern are even more clear near the boundary of cylinder. Fig.7 shows the temperature profile for the heat transfer through viscous dissipation at time 3s, it is clear from figure that value of temperature starts increasing as we move away from upper boundary towards the lower boundary. The maximum value of the temperature profile is this case is 301 kelvin that can been seen is the figure. Fig. 8 describes temperature distribution at time 1s as the result near the boundary of elliptic cylinder value of temperature is low while at upper and lower boundary the temperature has maximum value. Fig. 9 the isothermal contours of temperature are presented at time 3s, a unique pattern is obtained at this stage value of temperature profile has slightly decreased as observed from the figure. In this case maximum value of the temperature shift is 299 kelvin. Fig. 10 shows the isothermal contours at time 1s, the pattern is moving away from the cylinder as shown in the figure, in this case maximum temperature value is 298 kelvin.

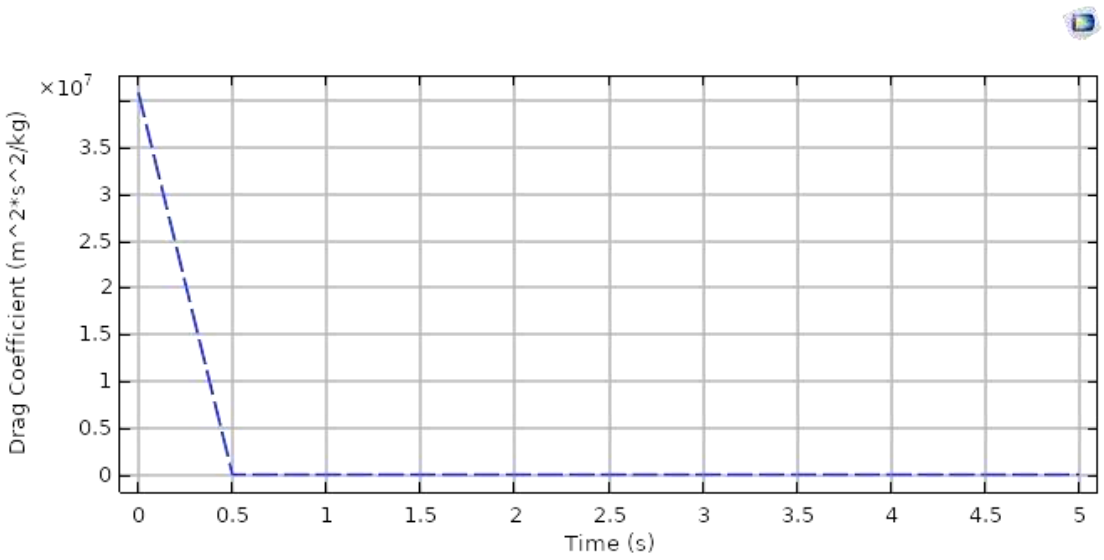

Fig. 11 Drag coefficient for laminar flow

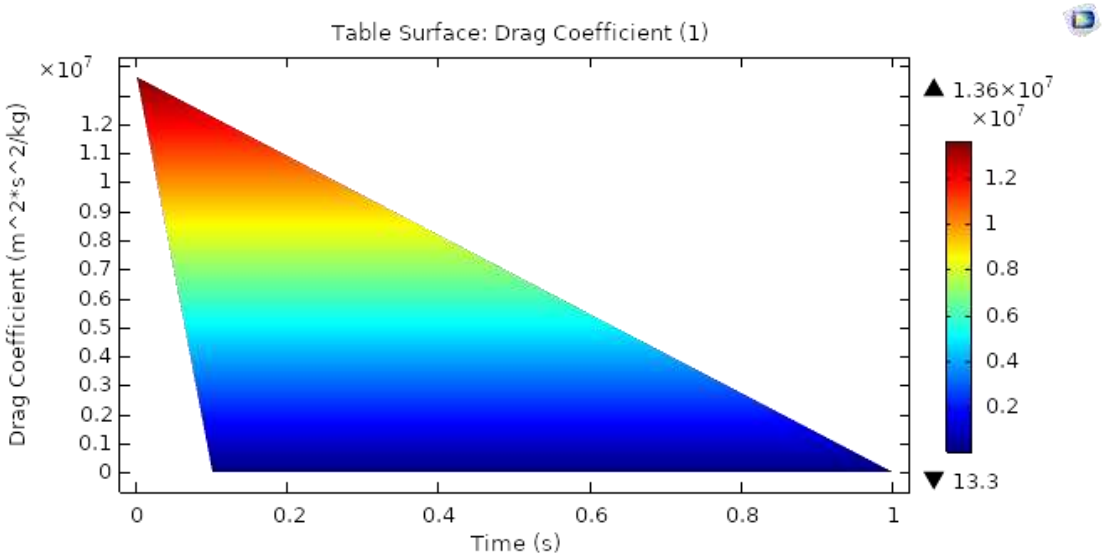

Fig. 12 Surface table of Drag coefficient for laminar flow

Fig. 11 shows drag coefficient behaviour for present problem, the drag force shows sudden decrease when the time scale reaches 0.5s, afterwards the drag force show constant linear behaviour. Fig. 12 describes the surface change drag coefficient, the drag force is maximum at time 0s as seen from table. The maximum value for drag is 1. 36.

5. Conclusions

Present results are discussed under the heat transfer influence, the model is time dependent. The model for present study has been modeled in COMSOL, the viscous compressible flow has shown distinct pattern for relevant parameters.

- The velocity distribution with heat transfer show varying distinctively for time dependent laminar flow
- Pressure distribution profile has also shown clear pattern but as we move away elliptic cylinder the pattern disappear because of varying time.
- The isothermal contours are very clear and distinct for each step of time.
- Drag coefficient has shown linear behaviour after very slight change of time.

6. References

[1]. Malik, M. Y., Hussain, A., & Nadeem, S. (2013). Boundary layer flow of an Eyring–Powell model fluid due to a stretching cylinder with variable viscosity. *Scientia Iranica*, *20*(2), 313-321.

[2]. Nadeem, S., Abbas, N., & Khan, A. U. (2018). Characteristics of three dimensional stagnation point flow of hybrid nanofluid past a circular cylinder. *Results in physics*, *8*, 829-835.

[3]. Nadeem, S., Rehman, A., Lee, C., & Lee, J. (2012). Boundary layer flow of second grade fluid in a cylinder with heat transfer. *Mathematical Problems in Engineering*, *2012*.

[4]. Naseer, M., Malik, M. Y., Nadeem, S., & Rehman, A. (2014). The boundary layer flow of hyperbolic tangent fluid over a vertical exponentially stretching cylinder. *Alexandria engineering journal*, *53*(3), 747-750.
[5]. Hussain, A., & Ullah, A. (2016). Boundary layer flow of a Walter's B fluid due to a stretching cylinder with temperature dependent viscosity. *Alexandria Engineering Journal*, *55*(4), 3073-3080.
[6]. Hussain, A., Afzal, S., Rizwana, R., & Malik, M. Y. (2020). MHD stagnation point flow of a Casson fluid with variable viscosity flowing past an extending/shrinking sheet with slip effects. *Physica A: Statistical Mechanics and Its Applications*, *553*, 124080.
[7]. Hussain, A., Sarwar, L., Akbar, S., Nadeem, S., & Jamal, S. (2019). Numerical investigation of viscoelastic nanofluid flow with radiation effects. *Proceedings of the Institution of Mechanical Engineers, Part N: Journal of Nanomaterials, Nanoengineering and Nanosystems*, *233*(2-4), 87-96.
[8]. Rehman, F. U., Nadeem, S., & Haq, R. U. (2017). Heat transfer analysis for three-dimensional stagnation-point flow over an exponentially stretching surface. *Chinese journal of physics*, *55*(4), 1552-1560.
[9].Vajravelu, K. (2001). Viscous flow over a nonlinearly stretching sheet. *Applied mathematics and computation*, *124*(3), 281-288.
[10].Lin, A., & Rubin, S. G. (1982). Three-dimensional supersonic viscous flow over a cone at incidence. *AIAA Journal*, *20*(11), 1500-1507.
[11].Van Driest, E. R. (1952). Calculation of the stability of the laminar boundary layer in a compressible fluid on a flat plate with heat transfer. *Journal of the Aeronautical Sciences*, *19*(12), 801-812.
[12].Malik, M. R., & Spall, R. E. (1991). On the stability of compressible flow past axisymmetric bodies. *Journal of fluid mechanics*, *228*, 443-463.
13].Kumar, B. R., & Sivaraj, R. (2013). Heat and mass transfer in MHD viscoelastic fluid flow over a vertical cone and flat plate with variable viscosity. *International Journal of Heat and Mass Transfer*, *56*(1-2), 370-379.
[14].Cantwell, B. J. (1996). Fundamentals of compressible flow.
[15].Barnoon, P., & Toghraie, D. (2018). Numerical investigation of laminar flow and heat transfer of non-Newtonian nanofluid within a porous medium. *Powder Technology*, *325*, 78-91.
[16].Yang, W., Lee, K. K., & Choi, S. (2017). A laminar-flow based microbial fuel cell array. *Sensors and Actuators B: Chemical*, *243*, 292-297.
[17].Zahid, S., Hobson, P. R., & Cockerill, D. J. A. (2018). Simulating multi-channel vacuum phototriodes using COMSOL. *Nuclear Instruments and Methods in Physics Research Section A: Accelerators, Spectrometers, Detectors and Associated Equipment*, *912*, 119-122.
[18].Houda, S., Belarbi, R., & Zemmouri, N. (2017). A CFD Comsol model for simulating complex urban flow. *Energy Procedia*, *139*, 373-378.
[19].Ahmad, M. F., Haniffah, M. R. M., Kueh, A., & Kasiman, E. H. (2020, April). Numerical study on drag and lift coefficients of a marine riser at high Reynolds number using COMSOL multiphysics. In *IOP Conference Series: Earth and Environmental Science* (Vol. 476, No. 1, p. 012075). IOP Publishing.
[20].Fröhlingsdorf, W., & Unger, H. (1999). Numerical investigations of the compressible flow and the energy separation in the Ranque–Hilsch vortex tube. *International Journal of Heat and Mass Transfer*, *42*(3), 415-422.
[21].Colonius, T. (2004). Modeling artificial boundary conditions for compressible flow. *Annu. Rev. Fluid Mech.*, *36*, 315-345.

[22].Zhou, X., Yang, J., Xiao, B., Hou, G., & Wu, Y. (2009). Numerical investigation of a compressible flow through a solar chimney. *Heat Transfer Engineering*, *30*(8), 670-676.
[23].Odenbach, S., & Thurm, S. (2002). Magnetoviscous effects in ferrofluids. In *Ferrofluids* (pp. 185-201). Springer, Berlin, Heidelberg.
[24].Bhandari, A., & Kumar, V. (2015). Effect of magnetization force on ferrofluid flow due to a rotating disk in the presence of an external magnetic field. *The European Physical Journal Plus*, *130*(4), 1-12.
[25].Bhandari, A. (2020). Effect of magnetic field dependent viscosity on the unsteady ferrofluid flow due to a rotating disk. *International Journal of Applied Mechanics and Engineering*, *25*(2), 22-39.
[26].Saleem, A., Qaiser, A., & Nadeem, S. (2020). Physiological flow of biomedical compressible fluids inside a ciliated symmetric channel. *Advances in Mechanical Engineering*, *12*(7), 1687814020938478.

Figures

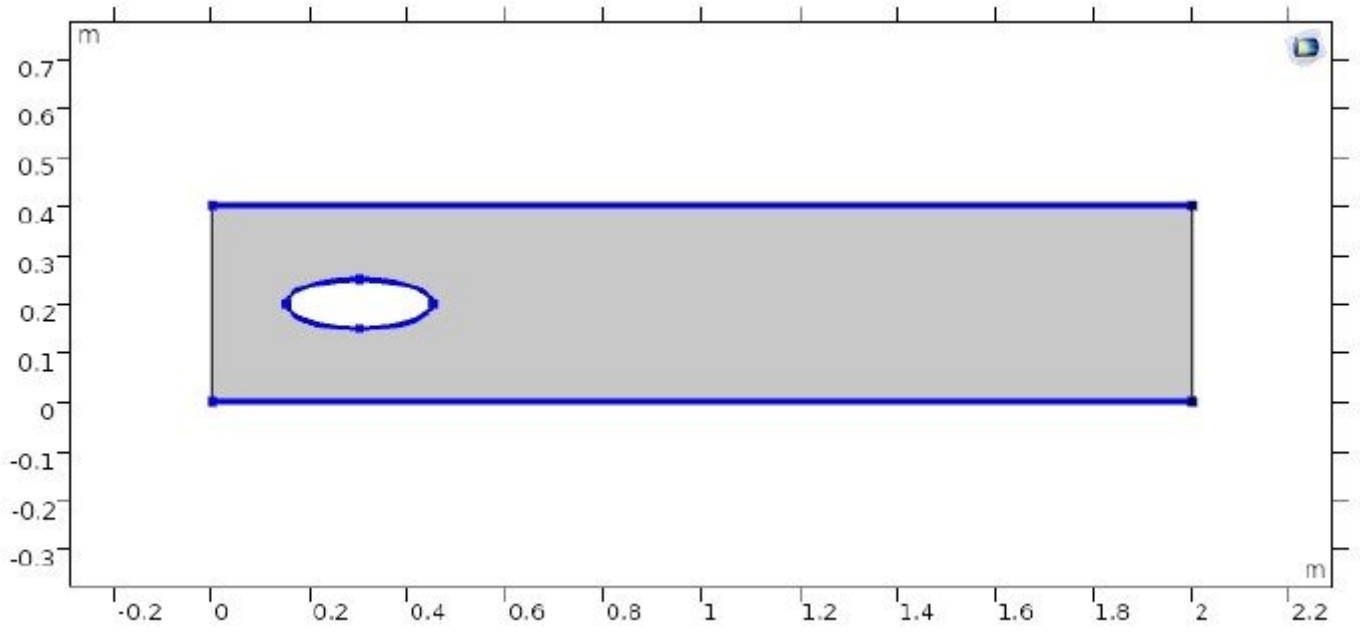

Figure 1

The sketch of two dimensional elliptic cylindrical flow.

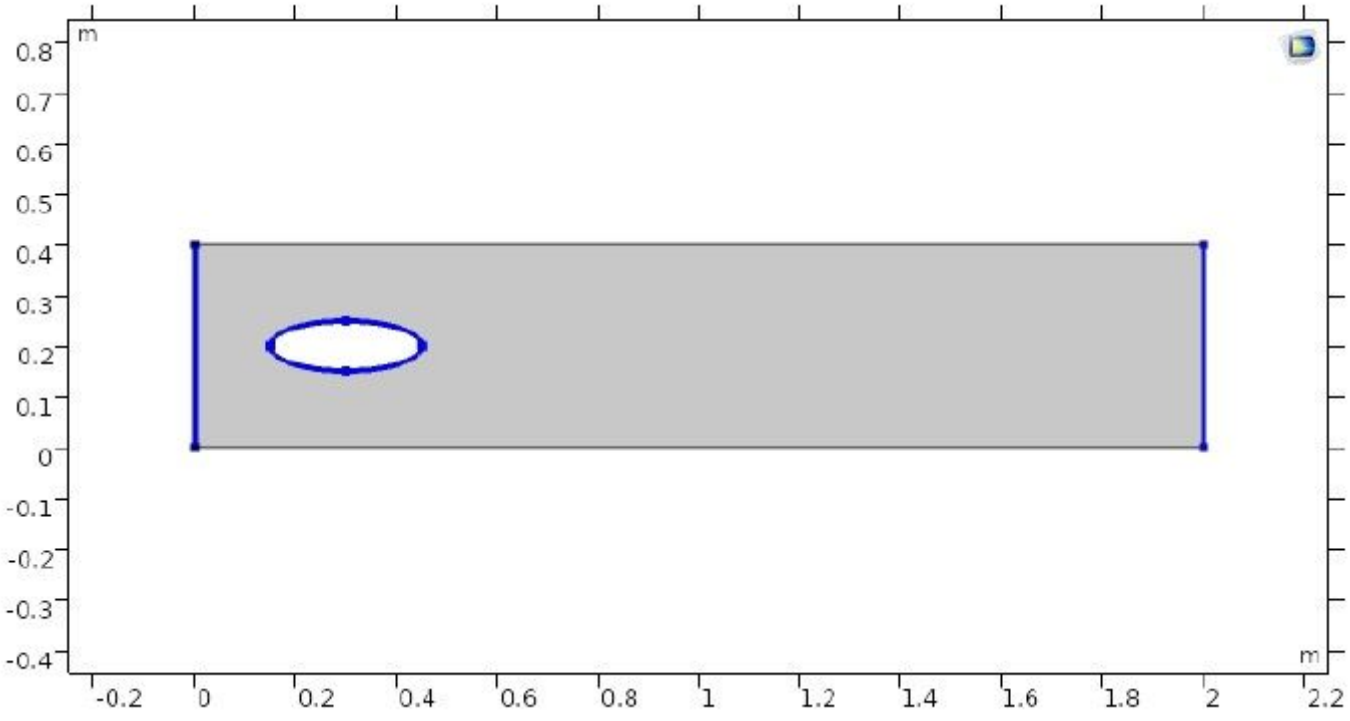

Figure 2

The sketch of thermal isolated boundary of two dimensional elliptic cylindrical flow.

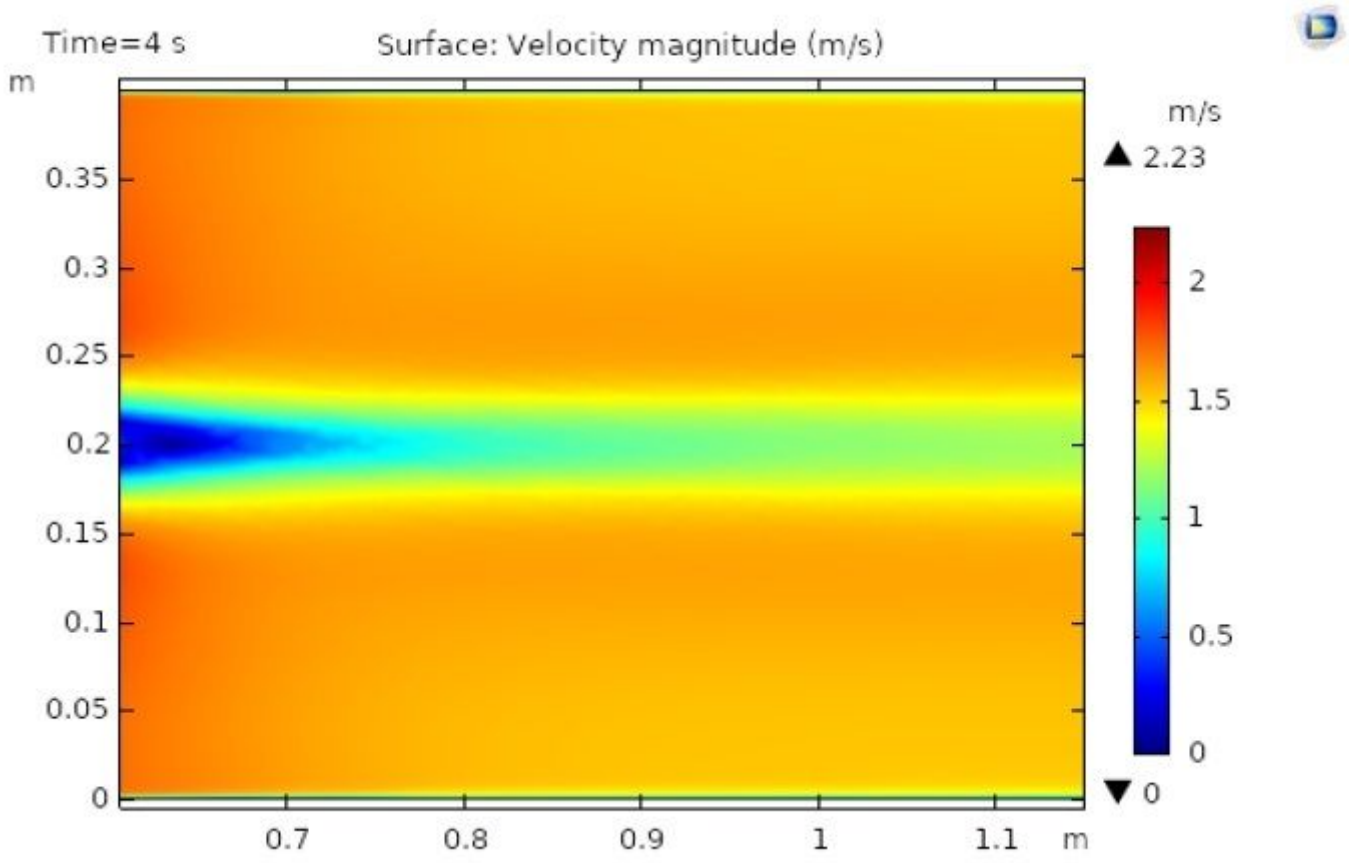

Figure 3

The velocity distribution in two dimensional elliptic cylindrical flow at t=4s

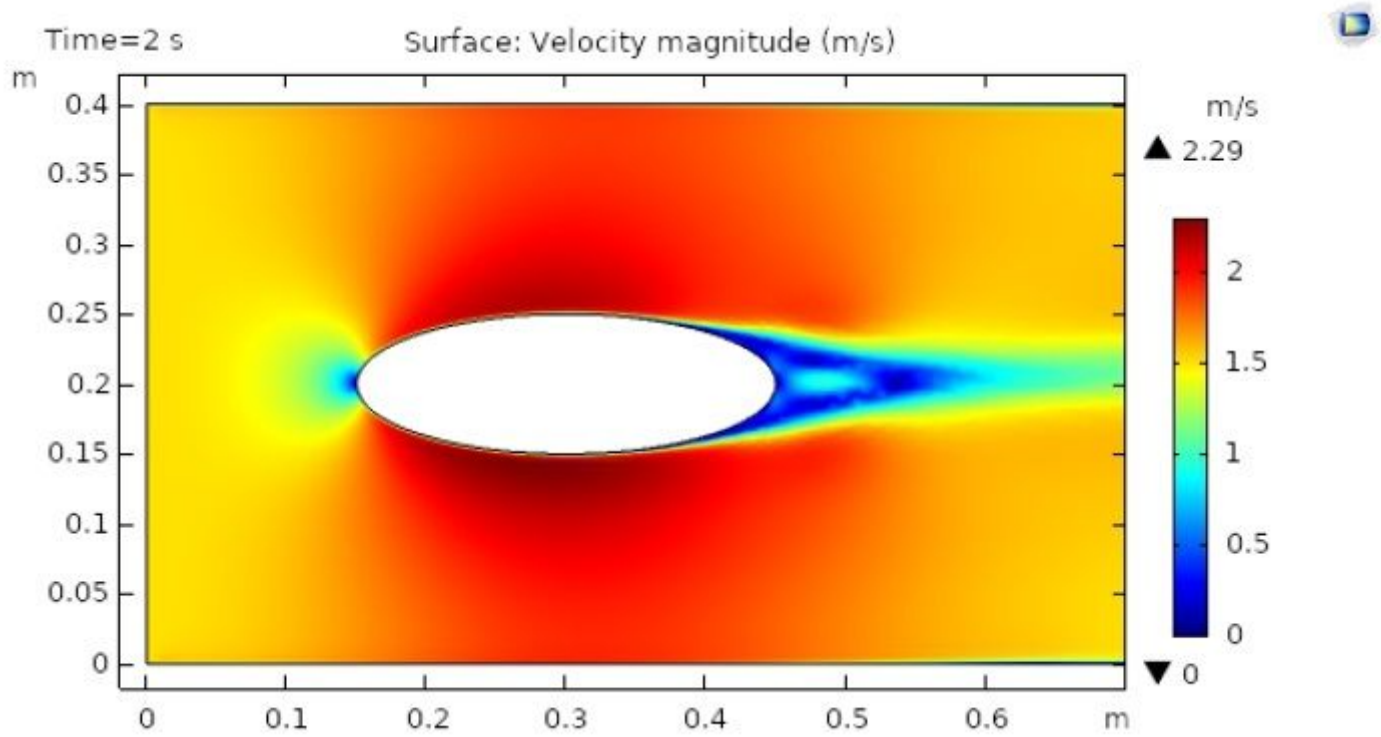

Figure 4

The velocity distribution in two dimensional elliptic cylindrical flow at t=2s

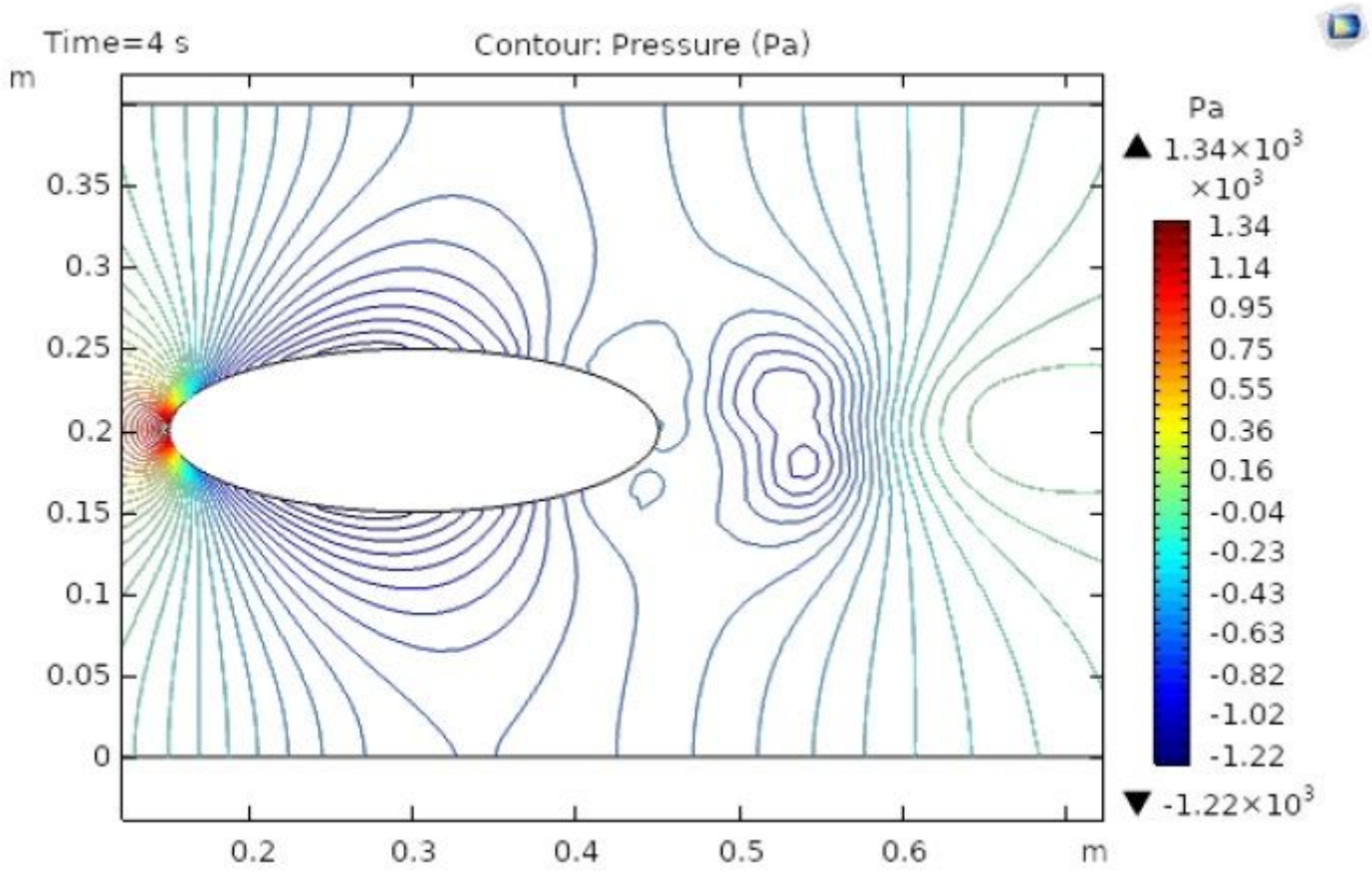

Figure 5

Pressure distribution in two dimensional elliptic cylindrical flow at t=4s

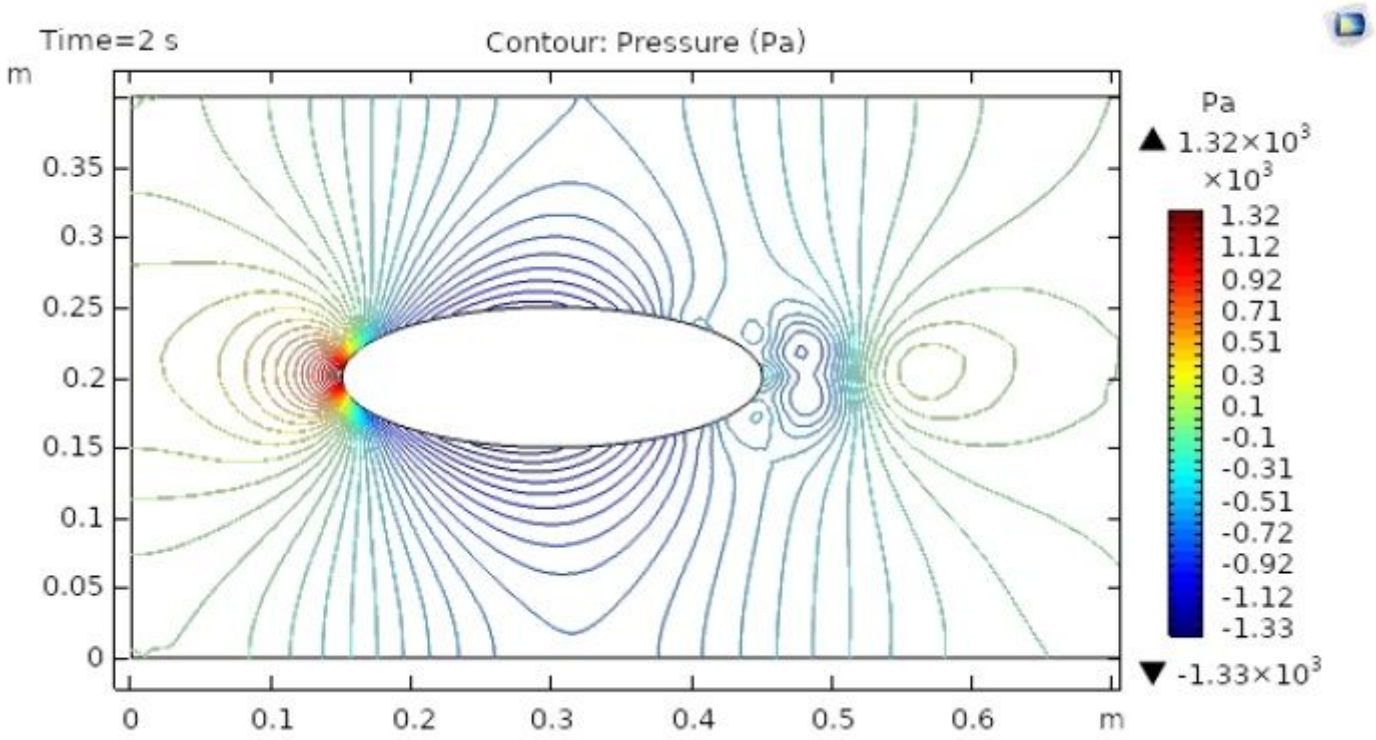

Figure 6

The pressure distribution in two dimensional elliptic cylindrical flow at t=2s

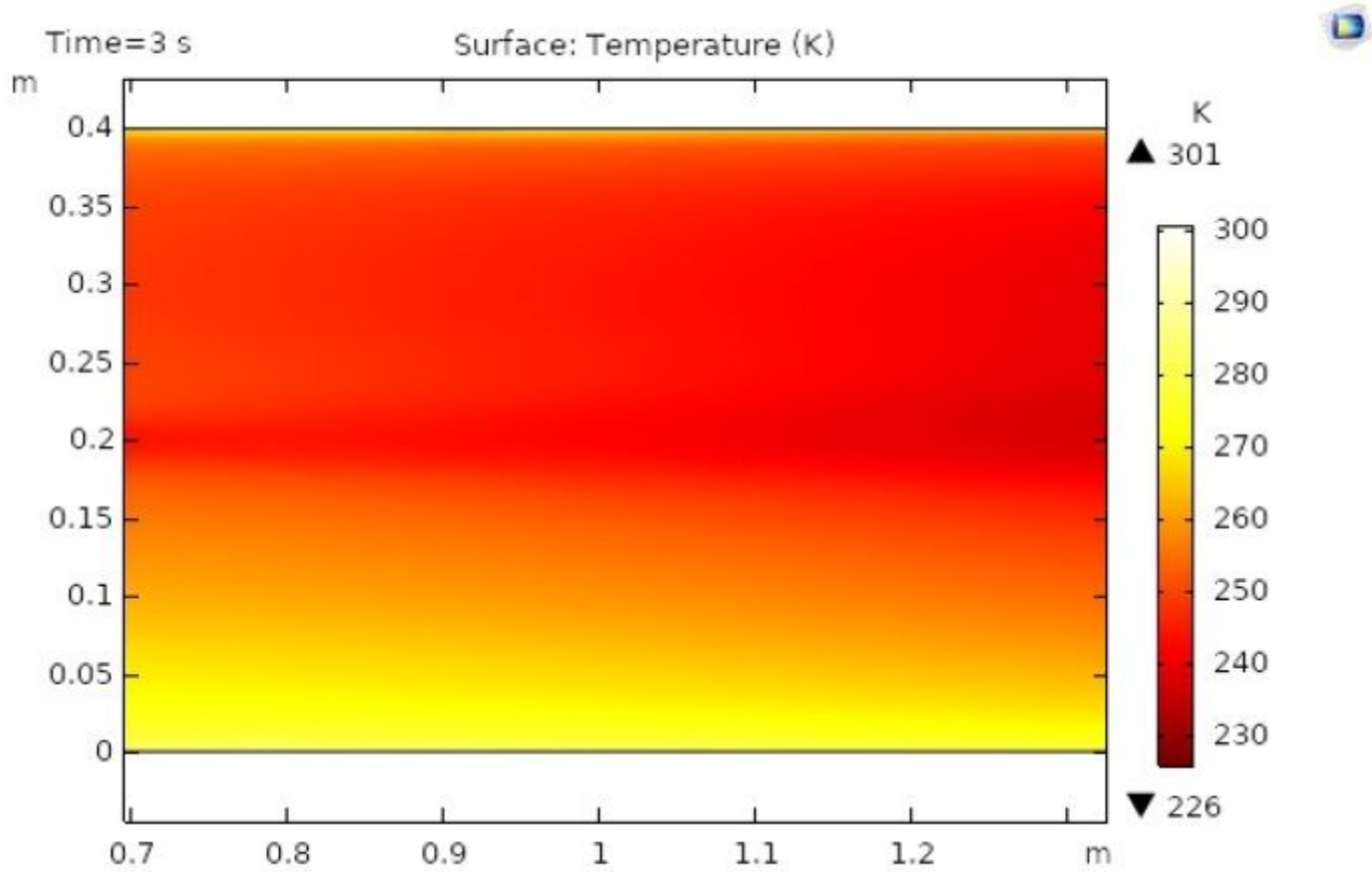

Figure 7

Temperature distribution at t=3s

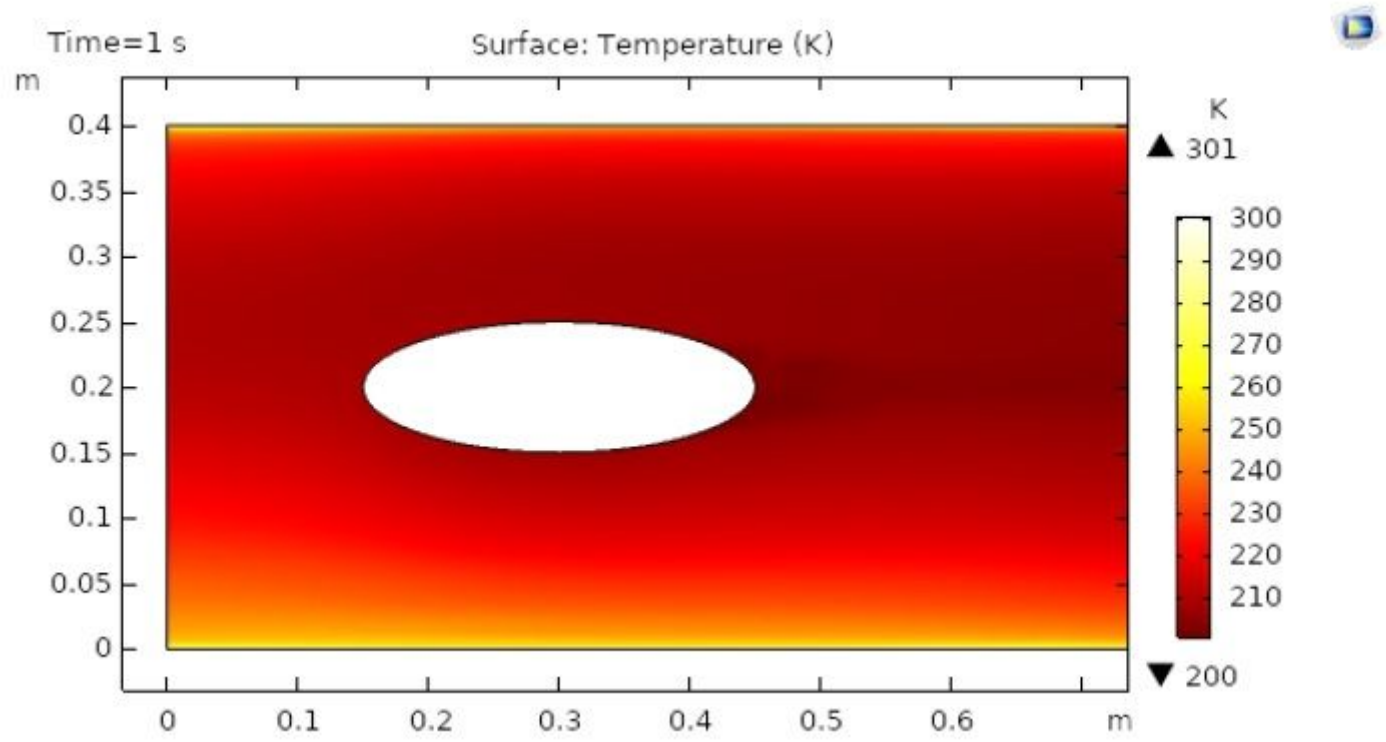

Figure 8

Temperature distribution at t=1s

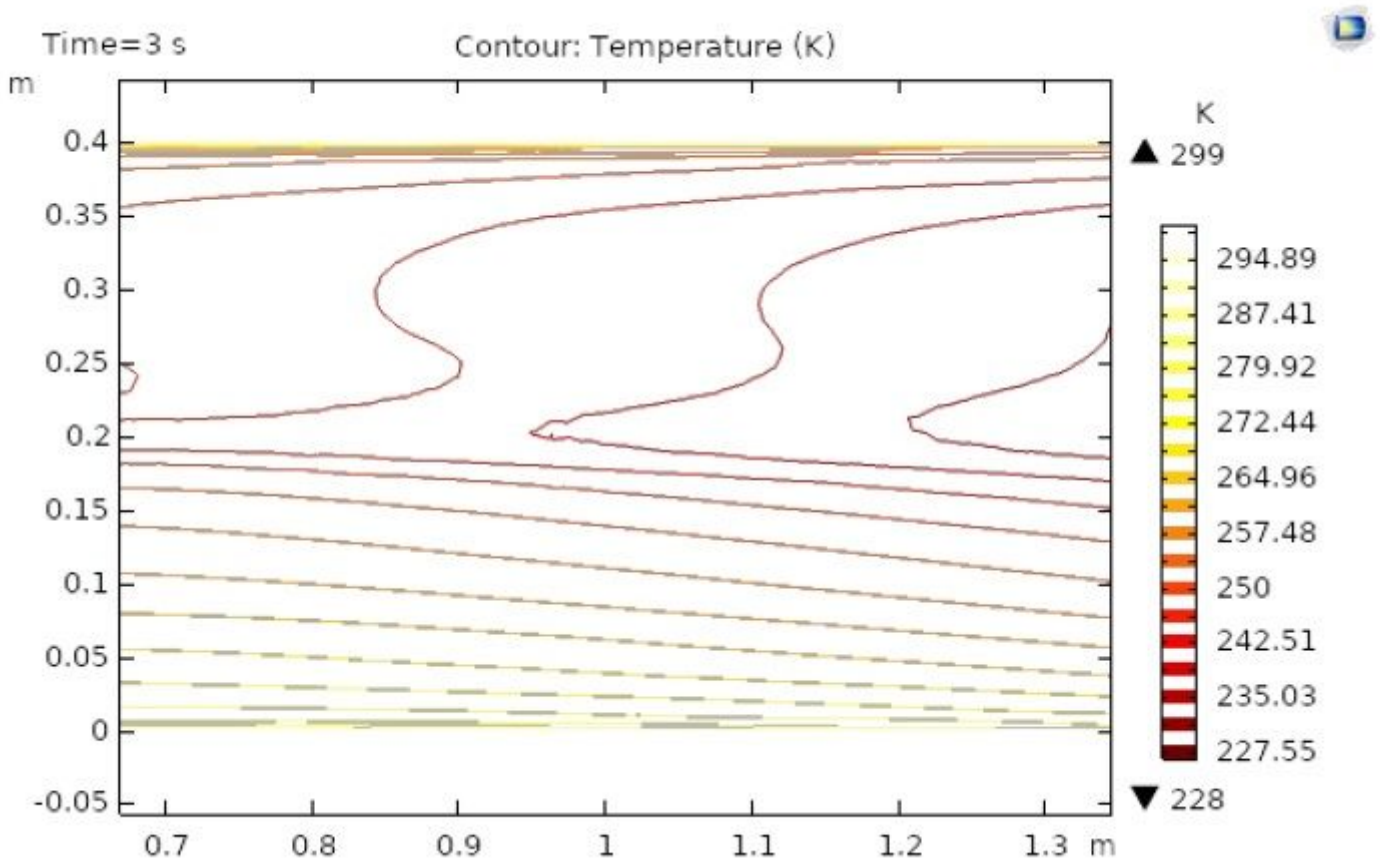

Figure 9

Isothermal contour temperature distribution at t=3s

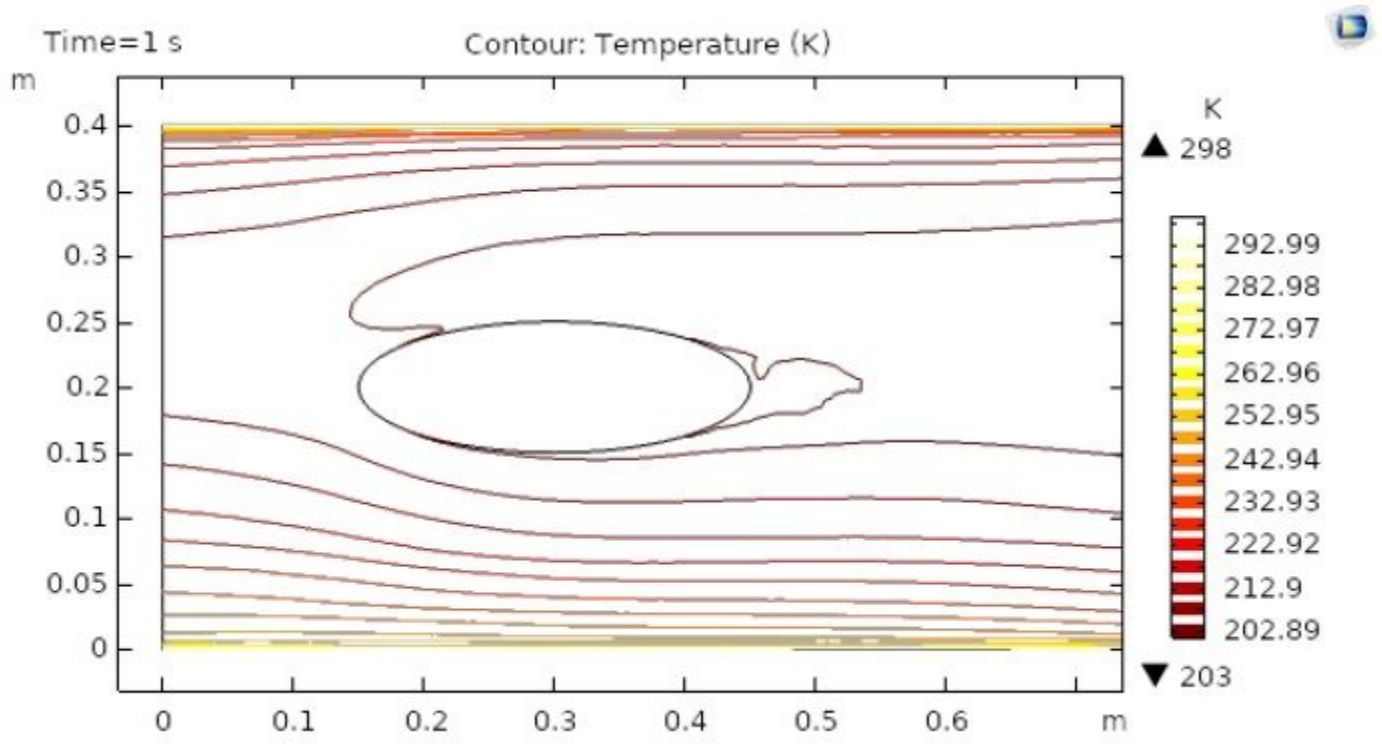

Figure 10

The velocity distribution in two dimensional elliptic cylindrical flow at t=1s

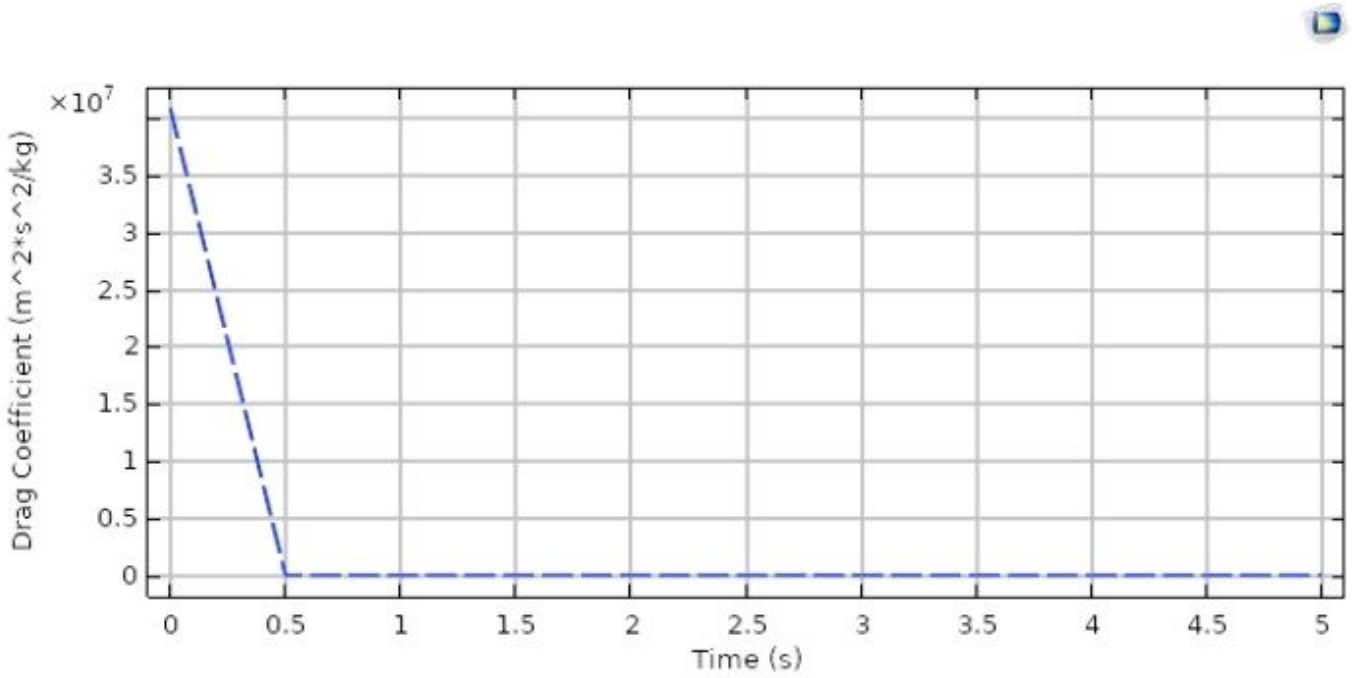

Figure 11

Drag coefficient for laminar flow

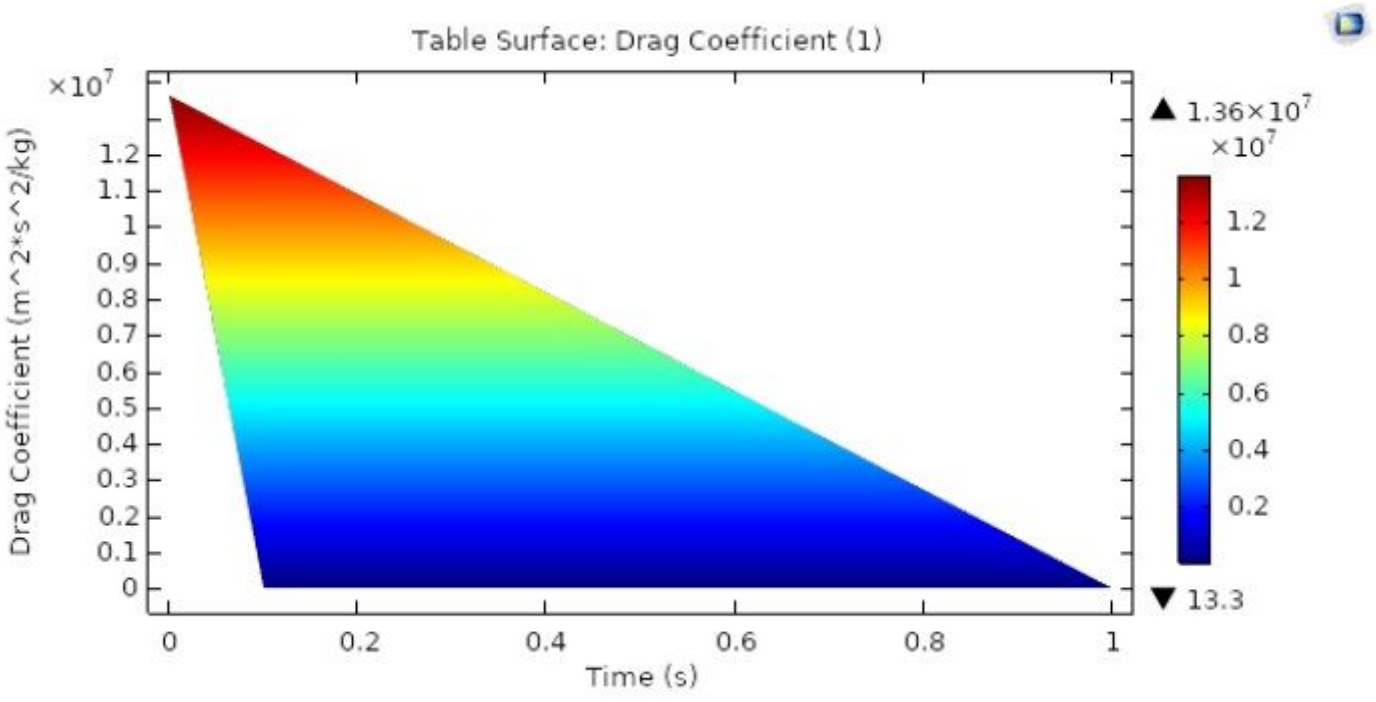

Figure 12

Surface table of Drag coefficient for laminar flow